

Development of Piezoelectric Gas Micro Pumps with the PDMS Check Valve Design

Chiang-Ho Cheng, An-Shik Yang, Hong-Yih Cheng, Ming-Yu Lai

Abstract—This paper presents the design and fabrication of a novel piezoelectric actuator for a gas micro pump with check valve having the advantages of miniature size, light weight and low power consumption. The micro pump is designed to have eight major components, namely a stainless steel upper cover layer, a piezoelectric actuator, a stainless steel diaphragm, a PDMS chamber layer, two stainless steel channel layers with two valve seats, a PDMS check valve layer with two cantilever-type check valves and an acrylic substrate. A prototype of the gas micro pump, with a size of 52 mm × 50 mm × 5.0 mm, is fabricated by precise manufacturing. This device is designed to pump gases with the capability of performing the self-priming and bubble-tolerant work mode by maximizing the stroke volume of the membrane as well as the compression ratio via minimization of the dead volume of the micro pump chamber and channel. By experiment apparatus setup, we can get the real-time values of the flow rate of micro pump and the displacement of the piezoelectric actuator, simultaneously. The gas micro pump obtained higher output performance under the sinusoidal waveform of 250 V_{pp}. The micro pump achieved the maximum pumping rates of 1185 ml/min and back pressure of 7.14 kPa at the corresponding frequency of 120 and 50 Hz.

Keywords—PDMS, Check valve, Micro pump, Piezoelectric.

I. INTRODUCTION

MICROPUMP is one of the important units in the application of microfluidic application. It has been designed to deliver small and precise volumes of gas or liquid. The advantages of MEMS micro pumps are due to their small-size, light weight and cost reduction. In addition, the technological development has been pushed toward lab-on-chip (LOC) methodologies, where a micro pump is used to deliver a small amount of liquid precisely in a large integrated system. The gas micro pumps have several significant advantages, such as small size, low power consumption, and portability, that are highly desirable in many emerging applications, including health and environmental monitoring [1], microelectronics cooling [2], micropropulsion [3], and power generation [4].

As a result, micro pumps have been an important topic for many researches as presented in several excellent reviewed papers discussing about the types of micro pumps, theory and principle of micro pumps, valve design, actuation methods,

materials and fabrication technologies, and microfluidic manipulation [5]-[10]. The actuation forms can be divided into two categories: mechanical and non-mechanical actuation in general. Since there are no moving elements, the structure of non-mechanical micro pumps is simpler than that of mechanical micro pumps. Mechanical micro pumps are relatively less sensitive to the gas properties as compared to those non-mechanical micro pumps. Mechanical micro pumps can be further classified into two categories according to valve types, which are valveless micro pumps [11], [12] and check valve micro pumps [13]. The structures of the valveless micro pumps are relatively simple; therefore, they are easy to be fabricated. However, the issues of backflow and random flow are not evitable for the valveless micro pumps. In contrast, the check valve micro pumps show better performance to manage the backflow and random flow problems; though the fabrication processes of most check valve micro pumps are more challenging and complex in general.

The operating pressures of polymers-made check valves are substantially lower than those made of silicon and metal because of small Young's modulus values of polymers materials as compared to those of silicon and metal. A softer polymeric material also offers much better sealing characteristics. Several works on polymeric check valves was presented, such as check valves were fabricated in polyimide [14], polyester [15], parylene [13], silicone rubber [16], SU-8 [17] and PDMS [18]. The PDMS has good processing and sealing properties with a comparatively lower Young's modulus value than other polymers. Accordingly, PDMS was used to fabricate the check valves in this study.

II. DESIGN

Fig. 1 shows a novel gas micro pump with check valve proposed in this study and its top view and the cross-section view of the structure on the AA section are shown in Figs. 2 and 3, respectively. The micro pump consists of several structural layers from bottom up: an acrylic substrate as the lower cover, two channel layer with a channel to introduce the driving pressure, a PDMS check valve layer with two cantilever-type check valves used to open or close the channel, a PDMS chamber layer to define the actuation area, a stainless steel diaphragm and a piezoelectric disc as the actuator. The first and second channel layers are identical. The space between the first channel layer and the chamber layer defines the pump chamber. During operations, the piezoelectric is first actuated by the positive voltage to direct the diaphragm away from the chamber causing a decrease of chamber pressure due to the volume

Chiang-Ho Cheng and Ming-Yu Lai are with the Department of Mechanical and Automation Engineering, Da-Yeh University, Changhua, 515, Taiwan (phone: (886) 4-8511888 ext. 2119; e-mail: chcheng@mail.dyu.edu.tw).

An-Shik Yang is with the Department of Energy and Refrigerating Air-Conditioning Engineering, National Taipei University of Technology, Taipei, 106, Taiwan (e-mail: asyang@ntut.edu.tw).

Hong-Yih Cheng is with the Department of Mechanical and Automation Engineering, Da-Yeh University, Changhua, 515, Taiwan (e-mail: honyi@mail.dyu.edu.tw).

enlargement. Then, the inlet valve opens with closing of the outlet valve, and the air is sucked into the chamber from the inlet port. Afterward, the piezoelectric is actuated by the negative voltage to make the diaphragm driven towards the chamber causing the volume shrinkage and the chamber pressure climb; thus, the inlet valve closes and the outlet valve opens with the air squeezed out of the chamber via the outlet port. As the piezoelectric is actuated periodically, the pumping medium is thus delivered from the inlet port to the outlet port continuously.

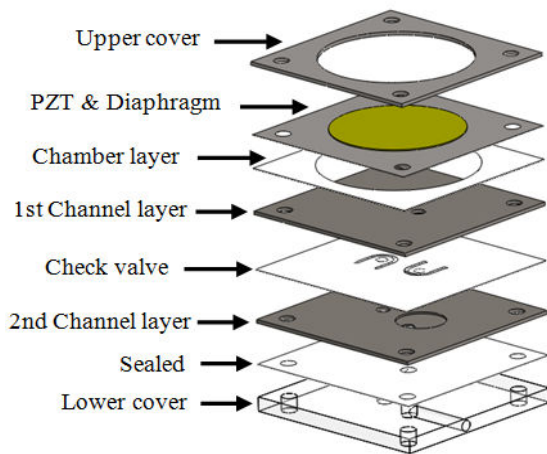


Fig. 1 Schematic of the micro pump with check valve

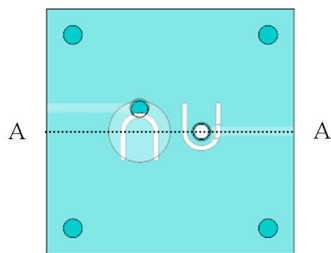


Fig. 2 The top view of the micro pump

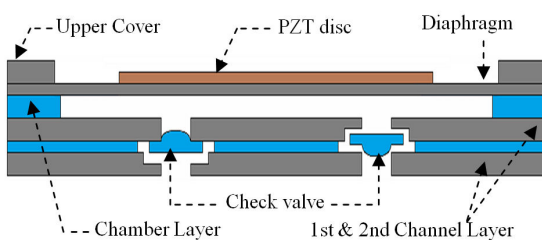


Fig. 3 The AA section view for the micro pump

III. FABRICATION

A. Channel and Upper Cover Layer

Two channel and upper cover layer were made of stainless steel substrate (52 mm × 52 mm × 1 mm in length, width and depth), which was fabricated by the MEMS-based lithography and wet etching process to form a circular cavity as the micro pump channel. An etchant consisting of 46g ferric chloride, 33g

hydrogen peroxide and 54g deionized water was utilized to obtain smooth uniform channels on the stainless steel substrates. At the start, the AZ 9260 photoresist was coated on the stainless-steel substrate by spin coater with both spreading step and thinning step. The photoresist on the substrate was baked on a hot plate or in an oven, and then exposed by a standard UV mask aligner (Karl Suss MA-6). The UV exposure process was performed under the hard contact mode with an intensity of 6 mW cm⁻² at a wavelength of 365 nm. The exposed photoresist was then developed in an immersion process via AZ400K diluted developer. Finally, the samples that were wet etched were immersed in the etchant at 53-58°C. The fabricated channel layer is shown in Fig. 4.

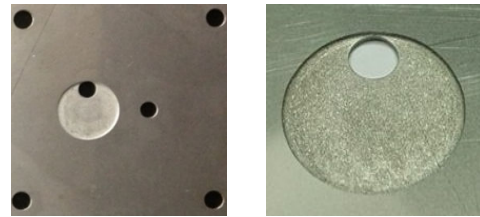


Fig. 4 The fabricated stainless steel channel layer

B. Lower Cover Layer

The lower cover layer was made of acrylic fabricated with the conventional CNC cutting and milling techniques. The acrylic plate was severed into the desired sizes (52mm×52mm×5mm in length, width and height) and micro-milled to form two vertical channels and two horizontal channels for the inlet and outlet.

C. Check Valve and Chamber Layer

The check valves and chamber were molded via a PDMS mixture. A 10:1 mixture of solution A and B supplied was stirred and degassed under the room temperature until the mixture became fully clear and bubble free. The solutions A and B work as the main agent and the coagulant, while the heating process can speed up solidification. Hence, the prepared PDMS mixture was poured onto the check valve's mold and cured at 75°C for 2h. After cooling, the products were taken out of the mould with great care so as to prevent damage to these very small and thin PDMS devices. The front view of check valve is shown in Fig. 5.

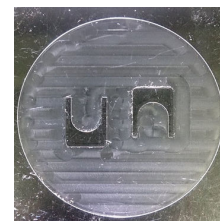


Fig. 5 Front view of check valve

D. Piezoelectric Actuator

The piezoelectric disc with 35 mm × 250 μm in diameter and thickness was prepared by the commercial available piezoelectric powder (SUNNYTEC Company, S54P5H type)

through the dry powder pressing technique. The sintering process was performed in a tube furnace under a quiescent air atmosphere at a heating rate of $90^{\circ}\text{C}/\text{min}$ to the peak temperatures of 1250°C for maintaining a duration of 2 hours, which followed by a $90^{\circ}\text{C}/\text{min}$ cooling rate to the room temperature. The poling electrodes were patterned using a screen-printing technique with silver paste. For poling the piezoelectric, the poling electric field was $2.0\text{V}/\mu\text{m}$ under the temperature of 100°C in 15 minutes. As shown in Fig. 6, the P-E hysteresis curves were measured by a high voltage test system (Radiant Technologies: Precision LC with HVI 10 kV). The coercive field (E_c) was $5.8\text{ kV}/\text{cm}$; the saturated polarization (P_s) and remnant polarization (P_r) were $38.04\mu\text{C}/\text{cm}^2$ and $31.7\mu\text{C}/\text{cm}^2$, respectively. Fig. 7 shows the measurement results for the d_{33} characteristics of the piezoelectric discs, the average value of d_{33} are $562.7\text{ pm}/\text{V}$ with standard deviation of 2.738.

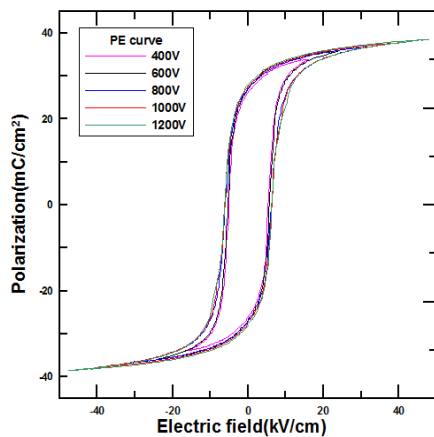


Fig. 6 P-E hysteresis curves of the Piezoelectric disc

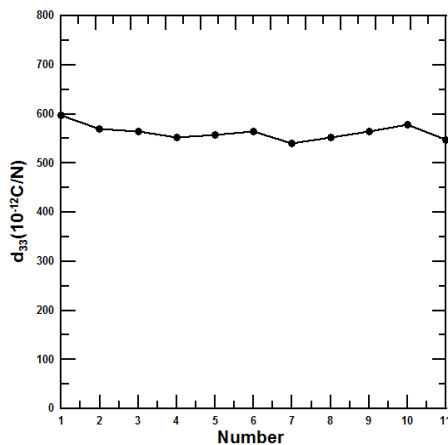


Fig. 7 d_{33} characteristics of the piezoelectric disc

E. Assembly

First, the epoxy adhesive (3M, DP-460) was applied on the attached surfaces by screen printing to assemble the diaphragm layer and piezoelectric actuator by the aligned marks in conjunction with a CCD aligning system. The adhesive was

cured in the oven kept at 60°C for 2 hours to prevent from depolarization. Finally, the stack of these layers (Upper cover, diaphragm, Chamber layer, 1st Channel layer, check valve layer, 2nd Channel layer and Lower cover) was fixed with four screws. The assembled device is shown in Fig. 8.

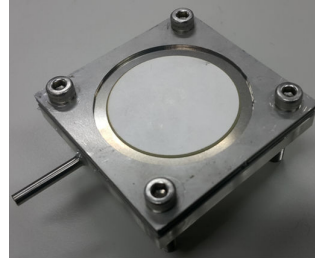


Fig. 8 The assembled gas micro pump

IV. EXPERIMENTAL APPARATUS

To understand the relation between the gas flow rate and the actuator displacement of the micro pump, we use the scanning laser vibrometer (Polytec MSV300) to measure the displacement and velocity of the piezoelectric actuator at the same time when the micro pump is actuated at different operating frequency. Each datum obtained is the average value from three measured samples with the same conditions. The deviations of the three measured values from the average must be within 5%. Fig. 9 shows the photograph of the experimental setup for the performance test of micro pump. The function generator (Agilent 33120A) generates the driving signal, which is amplified by the voltage amplifier (Trek Model 601C) to actuate the piezoelectric actuator. The micro pump is actuated to work and the mass flow meter with the precision of 0.1 ml is used to measure the gas flow rate. The real-time measurement system designed by a LabView software interface via the RS232 port is used to record the time history of gas flow rate.

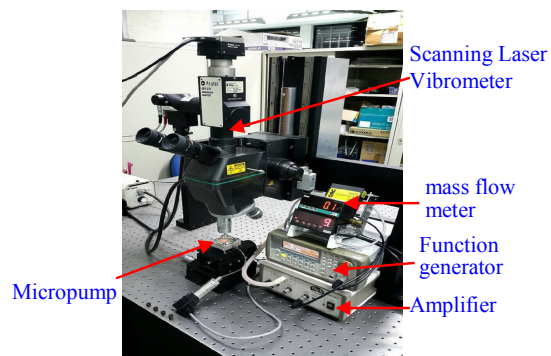


Fig. 9 Photograph of the experimental setup for the performance test of gas micro pump

V. PERFORMANCE OF MICRO PUMP

A. Performance of Flow Rate and Back Pressure

The micro pump was tested with air and driven with 250Vpp

voltage under 0.3 mm check valve thickness and 0.5 mm chamber depth. To better understand the relation between the air flow rate and the actuator displacement of the micro pump, we employed the scanning laser vibrometer to simultaneously measure the displacement of the piezoelectric center and air flow rate when the micro pump was actuated at different operating frequencies. Fig. 10 illustrates the displacement of the piezoelectric center at all operating frequencies for three different diaphragm thicknesses. When the actuation frequency was swept from 10 Hz to about 200 Hz, the displacement of piezoelectric actuator almost did not change with the actuation frequency. The frequency dependence of the pumping rate at zero back pressure is shown in Fig. 11 for three different diaphragm thicknesses (80, 100 and 120 μ m). The maximum pumping rates of 1185, 1080 and 1030 ml/min, respectively, were achieved at the frequency of 120 Hz. For all diaphragm thicknesses, the flow rate increased with the frequency and the peak was at 120 Hz; the flow rate decreased as the frequency beyond 120 Hz.

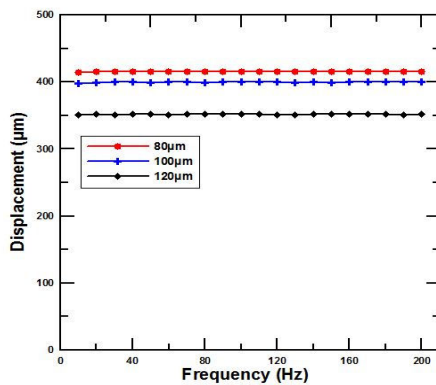


Fig. 10 The displacement of the piezoelectric center with respect to the frequency for three different diaphragm thicknesses

Fig. 12 illustrates the flow rate vs. the actuating frequency at three different check valve thicknesses under 80 μ m diaphragm thickness and 0.5 mm chamber depth. The maximum pumping rates of 1185, 928 and 794 ml/min, respectively, were achieved at the frequency of 120 Hz. For all check valve thicknesses, the flow rate increased with the frequency and the peak was at 120 Hz; the flow rate decreased as the frequency beyond 120 Hz. Fig. 13 illustrates the flow rate vs. the actuating frequency at three different chamber depth under 80 μ m diaphragm thickness and 0.3 mm check valve thickness. The maximum pumping rates of 1033, 1185 and 1115 ml/min, respectively, were achieved at the frequency of 120Hz. Fig. 14 shows the relation between the frequency and the back pressure for three different diaphragm thickness with 0.5 mm chamber depth and 0.3mm check valve thickness. There are three peaks of backpressure for all three different check valves, whose thickness are 80, 100 and 120 μ m. The peak is at 50 Hz and the maximal back pressure of 6.43, 6.73 and 7.14kPa produced by the diaphragm with thickness of 80, 100 and 120 μ m, respectively.

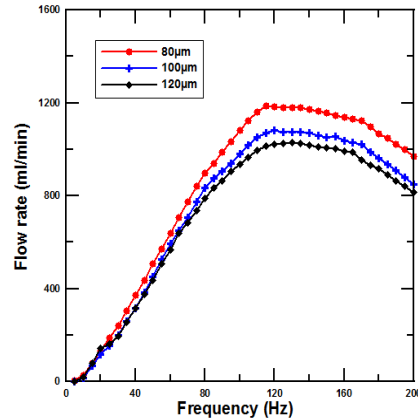


Fig. 11 Measured gas flow rate versus operating frequency for three different diaphragm thicknesses

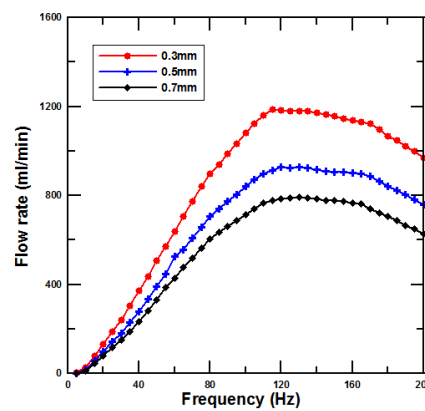


Fig. 12 Measured gas flow rate versus operating frequency for three different check valve thicknesses

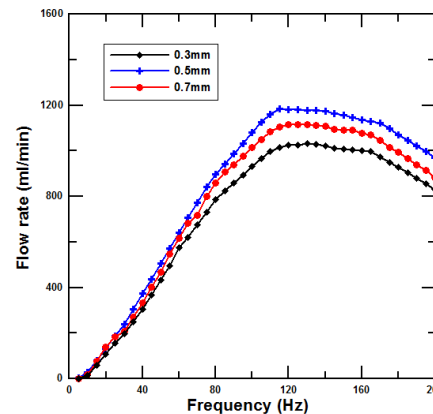


Fig. 13 Measured gas flow rate versus operating frequency for three different chamber depths

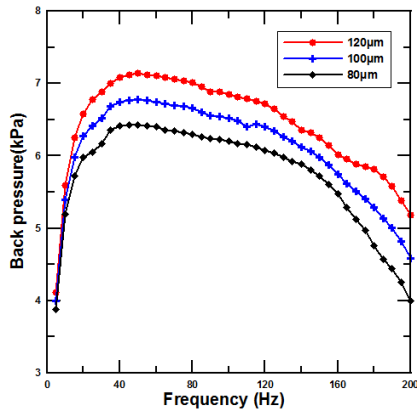


Fig. 14 Measured back pressure versus operating frequency for three different diaphragm thicknesses

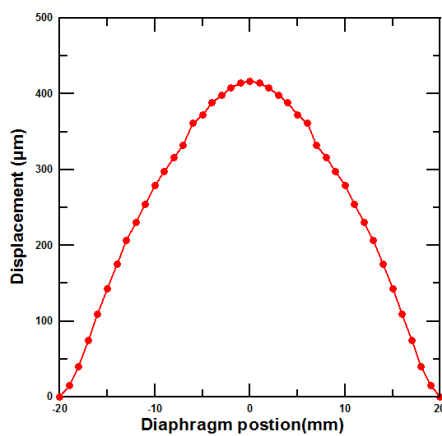


Fig. 15 The displacement of the piezoelectric actuator with respect to the diaphragm position in the radial direction

B. Pumping Efficiency

To understand the relation between the air flow rate of micro pump and the stroke volume rate of the piezoelectric actuator, we imposed a driving voltage signal, having the amplitude and frequency of 250Vpp and 120 Hz, on the pump with an 80 μm diaphragm thickness to measure diaphragm deformation. Fig. 15 presents the displacement of the piezoelectric actuator, measured by scanning laser vibrometer (Polytec MSV300), with respect to the diaphragm position in the radial direction. The stroke volume of the pump was about $2.258 \times 10^{-7} \text{ m}^3$, with the average area A_m and center peak displacement of $5.428 \times 10^{-4} \text{ m}^2$ and $4.16 \times 10^{-4} \text{ m}$. To compare the delivered flow rate of the micro pump from the stroke volume per minute for the piezoelectric actuator, we can multiply the displacement of piezoelectric actuator in Fig. 10 with the average area A_m to obtain the stroke volume rate (ml/min) under actuation. Figs. 16-18 show the comparison of the measured flow rate with the stroke volume rate (theoretical flow rate) for the diaphragm with the thickness of 80, 100 and 120 μm. From resulting experiments, the gas micro pump with the different diaphragm all have the similar the relation between measured flow rate and the theoretical flow rate. That is, the flow rate is proportion to

the displacement. The flow rate is the bigger as the piezoelectric actuator produces the larger displacement. From Figs. 16-18, the results indicate that the flow rate of the micro pump is much smaller than the stroke volume rate of the piezoelectric actuator at the frequency exceeding 120Hz. This is because the frequency is over the system's bandwidth with larger frequencies resulting in worse efficiencies in operation. From the curves in Figs. 16-18, the pumping efficiency was obtained via dividing the experimental flow rate by the stroke volume rate. The relation between the pumping efficiency and the frequency/voltage of actuation for three different diaphragm thicknesses is shown in Fig. 19. The peak is at 80 Hz and the maximal pumping efficiency of 82.7, 80.9 and 86.0 % produced by the diaphragm with thickness of 80, 100 and 120 μm, respectively.

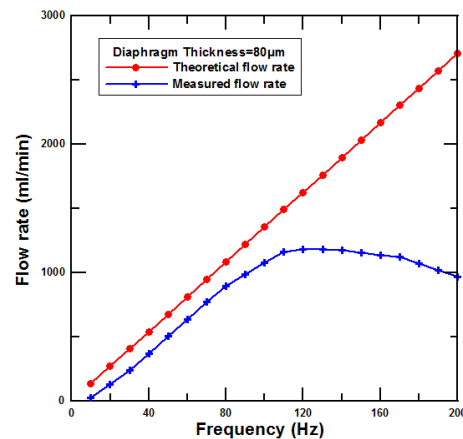


Fig. 16 The relationship between the measured flow rate and the theoretical flow rate of the piezoelectric actuator with the diaphragm thickness of 80 μm

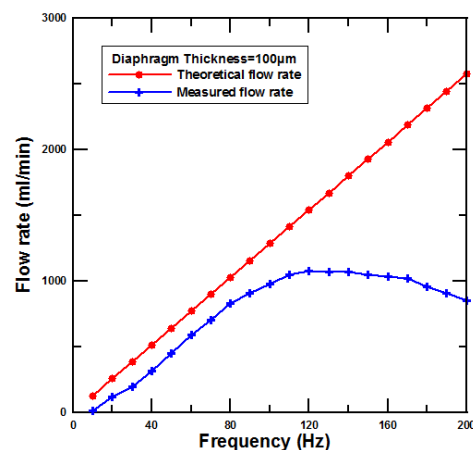


Fig. 17 The relationship between the measured flow rate and the theoretical flow rate of the piezoelectric actuator with the diaphragm thickness of 100 μm

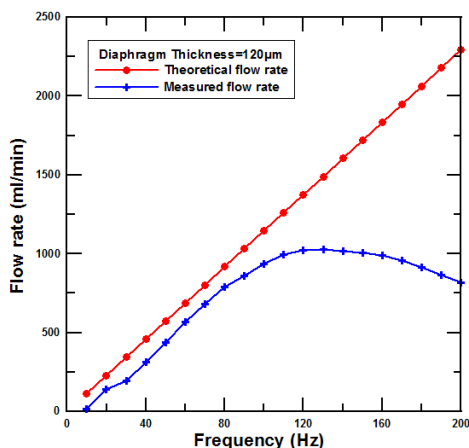


Fig. 18 The relationship between the measured flow rate and the theoretical flow rate of the piezoelectric actuator with the diaphragm thickness of $120\ \mu\text{m}$

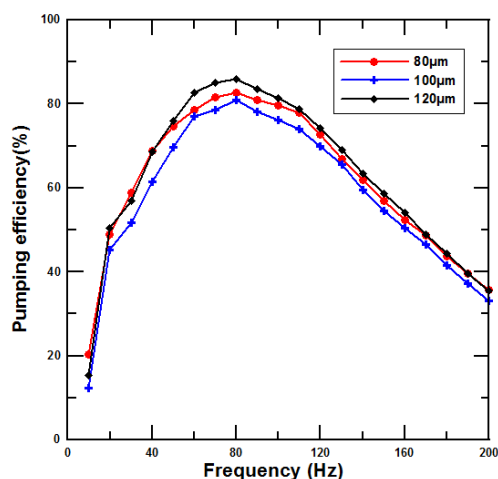


Fig. 19 The displacement of the piezoelectric center with respect to the frequency

VI. CONCLUSION

This paper described the design, fabrication and test of a check valve embedded micro pump for pumping gas. The micro pump is designed to pump gases with the capability of performing the self-priming and bubble-tolerant work mode by maximizing the stroke volume of the membrane as well as the compression ratio via minimization of the dead volume of the micro pump chamber and channel. The micro pump with check valve $0.3\ \text{mm}$ in thickness and chamber $0.5\ \text{mm}$ in depth obtained higher output performance under the sinusoidal waveform of $250\ \text{Vpp}$. The micro pump achieved the maximum pumping rates of $1185\ \text{ml/min}$ and back pressure of $7.14\ \text{kPa}$ at the corresponding frequency of 120 and $50\ \text{Hz}$.

ACKNOWLEDGMENT

The authors would like to thank the National Science Council of the Republic of China, Taiwan for financially supporting this

research under Contract No. NSC103-2221-E-212-016.

REFERENCES

- [1] H Kim, W H Steinecker, G R Lambertus, A A Astle, K Najafi, E T Zellers, L Bernal, P Washabaugh, K D Wise, "Integrated high-pressure 4-stage micro pump for high speed micro chromatography," Proc. 10th Int. Conf. Miniaturized Systems for Chemistry and Life Science (uTAS '06), Tokyo, Japan, pp. 1037-1039, 2006.
- [2] P Rodgers, V Evely, M Pecht, "Extending the limits of aircooling in microelectronic equipment," Proc. 6th Int. Conf. Thermal, Mechanical and Multiphysics Simulation and Experiment in Micro-electronics and Micro-systems, EuroSimE, Berlin, Germany, pp. 695-701, 2005.
- [3] Y Wang, G Yuan, Y K Yoon, M G Allen, S A Bidstrup, "Large eddy simulation (LES) for synthetic jet thermal management," Int. J. Heat Mass Transfer, Vol. 49, pp. 2173-2179, 2006.
- [4] L Arana, S Schaevitz, A Franz, M A Schmidt, K F Jensen, "A microfabricated suspended-tube chemical reactor for thermally efficient fuel processing," J. Microelectromech. Syst. Vol. 12, pp. 600-612, 2003.
- [5] N T Nguyen, X Huang and T K Chuan, "MEMS-micro pumps: a review," ASME J. Fluids Eng. Vol. 124, pp. 384-392, 2002.
- [6] D J Laser and J G Santiago, "A review of micro pumps," J. Micromech. Microeng. Vol. 14, pp. R35-R64, 2004.
- [7] P Woias, "Micro pumps-past, progress and future prospects," Sensors Actuators B Vol. 105, pp. 28-38, 2005.
- [8] H Kim, K Najafi, L P Bernal, "Gas micro pumps," in: Y. Gianchandani, O. Tabata, H. Zappe (Eds.), Comprehensive Microsystems, vol. 2, Elsevier Ltd., The Netherlands, pp. 273-299, 2008.
- [9] L Chen, S Lee, J Choo and E K Lee, "Continuous dynamic flow micro pumps for microfluid manipulation," J. Micromech. Microeng. Vol. 18, pp. 1-22, 2008.
- [10] F Amirouche, Y Zhou and T Johnson, "Current micro pump technologies and their biomedical applications," Microsyst. Technol. Vol. 15 pp. 647-666, 2009.
- [11] H Andersson, W van der Wijngaart, P Nilsson, P Enoksson and G Stemme, "A valve-less diffuser micro pump for microfluidic analytical systems," Sensors Actuators B Vol. 72, pp. 259-265, 2001.
- [12] B Fan, G Song and F Hussain, "Simulation of a piezoelectrically actuated valveless micro pump," Smart Mater. Struct. Vol. 14, pp. 400-405, 2005.
- [13] J Kang, J V Mantese and G W Auner, "A self-priming, high performance, check valve diaphragm micro pump made from SOI wafers," J. Micromech. Microeng. Vol. 18, pp. 1-8, 2009.
- [14] R. Rapp, W K Schomburg, D. Maas, J. Schulz and W. Stark, "LIGA micro pump for gases and liquids," Sens. Actuators A Vol. 40, pp. 57-61, 1994.
- [15] S Boehm, W Olthuis and P Bergveld, "A plastic micro pump constructed with conventional techniques and materials," Sensors Actuators A Vol. 77, pp. 223-228, 1999.
- [16] S. Santra, P. Holloway, D. Batich, "Fabrication and testing of a magnetically actuated micro pump," Sens. Actuators B Vol. 87, pp. 358-364, 2002.
- [17] T Q Truong and N T Nguyen, "A polymeric piezoelectric micro pump based on lamination technology," J. Micromech. Microeng. Vol. 14, pp.632-638, 2004.
- [18] J H Kim, K T Lau, R. Shepherd, Y Wu, G Wallace and D Diamond, "Performance characteristics of a polypyrrole modified polydimethylsiloxane (PDMS) membrane based microfluidic pump," Sensors and Actuators A Vol. 148, pp. 239-244, 2008.